TESTBED FOR NON-COHERENT ZERO-FEEDBACK DISTRIBUTED BEAMFORMING

George Sklivanitis *Konstantinos Alexandris* *Aggelos Bletsas*

Department of Electronic & Computer Engineering
Technical University of Crete, Chania, 73100, Greece
E-mail:{gsklivanitis, aggelos}@telecom.tuc.gr, kalexandris@isc.tuc.gr

ABSTRACT

We present the setup of a complete software-defined radio (SDR) testbed for non-coherent zero-feedback distributed beamforming. Three custom-built, embedded RF transceivers along with a commodity, low-cost SDR commercial receiver are deployed in an indoors lab environment. In sharp contrast with prior art on collaborative beamforming, the proposed scheme assumes *no feedback* between receiver and transmitters and no access to the transmitters' local oscillators for carrier phase adjustments. Quite interestingly, frequency offsets are exploited in this work. Zero-feedback beamforming with unsynchronized carriers is experimentally validated in terms of bit-error-rate (BER) and compared with simulation results. To the best of our knowledge, this is the first testbed for demonstrating and evaluating *zero-feedback*, channel state information (CSI)-free, distributed beamforming.

Index Terms— Distributed beamforming, emergency radio, zero-feedback, software-defined radios, wireless sensor networks.

1. INTRODUCTION

In collaborative beamforming wireless nodes cooperatively transmit their signals in a way that their phases align and constructively offer a beamforming gain towards the desired receiver. In contrast with traditional beamforming literature and classic phased-array systems, deployed terminals are distributed at random locations and operate as independent processing units. In that case, several challenges, such as different carrier frequency offsets and time synchronization between the distributed terminals have to be taken into account.

Recent theoretical and implementation works towards that research direction have mainly focused on receiver-feedback schemes [1]. Several proposed techniques [2–8] employ various types of feedback (i.e., pilot signals, digital links) for time and frequency synchronization issues. Authors in [9–11] introduce intermediate relay nodes with adaptively changing weights as a solution to the problems of the distributed setup. However, [9, 10] assume that relays have perfect knowledge of the transmit and receive channel state information (CSI), while all of them assume that feedback is available. By restricting the number of beamformers and choosing only a few of them, authors in [12] exploit CSI, based on receiver's feedback. The architecture presented in [3], revisited in [13] and implemented using software-defined radio (SDR) devices in [4–6], focuses on algorithms for frequency synchronization and phase alignment as well as advanced feedback methods. Finally, in [14, 15] authors suggest a difficult to implement scheme of exchanging round-trip messages in order to acquire CSI.

Contrary to the aforementioned prior art, we assume *no* specialized hardware for carrier or phase synchronization, *no* CSI availability, and *zero-feedback* between receiver and distributed transmitters. We were mainly motivated by scenarios where a reliable feedback channel is not feasible (e.g., reachback communication). Quite interestingly, inevitable frequency offsets, typically undesired in classic beamforming approaches, are exploited in this work. The idea is experimentally validated in terms of bit-error-rate (BER), in a low-cost testbed consisting of three custom-built embedded transmitters and a commercial SDR receiver, all equipped with inexpensive, commodity oscillators. To the best of our knowledge, the deployed testbed for evaluating *zero-feedback* collaborative beamforming is the first of its kind.

2. SYSTEM MODEL AND BASIC IDEA

In this paper, we consider a setup of M distributed ultra low-cost terminals, transmitting in a symbol-synchronized fashion to a SDR receiver. We denote by $x[k]$ the binary data symbol transmitted by all terminals at the k^{th} channel use, and by Δf_m the carrier frequency offset (CFO) component at the m^{th} user terminal, $m = 1, 2, \ldots, M$. Signals are considered to propagate through Rayleigh flat fading channels and experience additive complex white Gaussian noise (CWGN).

After carrier demodulation, matched filtering, estimation and correction of coarse CFO between receiver and transmitters and sampling at symbol transmission rate $1/T_s$, the re-

This research has been co-financed by the European Union (European Social Fund - ESF) and Greek national funds through the Operational Program "Education and Lifelong Learning" of the National Strategic Reference Framework (NSRF) - Research Funding Program: *Thales. Investing in knowledge society through the European Social Fund.*

ceived baseband signal can be represented as

$$y[k] \triangleq \sum_{m=1}^{M} h_m \, e^{+j2\pi\Delta f_m kT_s} \, x[k] + w[k] = \widetilde{x[k]} + w[k],$$

where $\widetilde{x[k]} \triangleq x[k] \sum_{m=1}^{M} A_m \exp\{+j(2\pi\Delta f_m kT_s + \phi_m)\}$, $h_m \triangleq A_m e^{j\phi_m} \sim \mathcal{CN}(0,1)$, is the wireless channel coefficient between m^{th} terminal and receiver and finally, $w[k] \sim \mathcal{CN}(0, \sigma^2)$.

By setting up a low-cost testbed for proving the concept of zero-feedback beamforming, carrier frequency offsets emerge between distributed transmitters and receiver. However, this challenge can be turned into an advantage [16] if the transmitted signals are viewed as rotating phasors $A_m \exp\{+j(2\pi\Delta f_m kT_s + \phi_m)\}$ at different speeds. Rotating speeds are contingent to varying carrier frequency offsets $\{\Delta f_m\}_{m=1}^{M}$. During different transmissions there will be a time section where signals align and offer a beamforming gain, assuming that channel remains constant for $L = \frac{\tau_c}{T_s}$ symbols.

In this work we exploit two different schemes of transmission in order to achieve the beamforming gains: i) repetition coding and ii) interleaving.

2.1. Repetition Coding

Repetition coding technique is based on retransmitting the same symbol for more than one, say L, consecutive symbol periods during the channel coherence time. The probability of signal alignment as a function of M, as well as the expected number of symbols where such zero-feedback beamforming gains occur, are analytically described in [16]. In that case, as shown in [17], the length-L received vector representation is

$$\mathbf{y} \triangleq \breve{\mathbf{h}} x + \mathbf{w} \tag{1}$$

where $\breve{\mathbf{h}} = \begin{bmatrix} \breve{h}_1 & \ldots & \breve{h}_L \end{bmatrix}^T$, $\mathbf{w} = \begin{bmatrix} w_1 & \ldots & w_L \end{bmatrix}^T$, $\breve{h}_l \triangleq \sum_{m=1}^{M} h_m \exp\{+j2\pi\Delta f_m lT_s\} \sim \mathcal{CN}(0, M)$, and $w_l \sim \mathcal{CN}(0, \sigma^2)$ for any set of CFO parameters $\{\Delta f_m\}_{m=1}^{M}$ and $l = 1, \ldots L$. Notice that given $\{\Delta f_m\}_{m=1}^{M}$, $\breve{h}_l$'s, for $l = 1, \ldots, L$, are proved to be n.i.i.d [17].

2.2. Interleaving

In this scheme, time domain is divided into N phases. On each phase, L information symbols, for which the channel remains unchanged, are transmitted. Thus, a length-N block is received for each symbol. In [17], channel taps corresponding to different phases have proved to be statistically independent. The employed technique is called interleaving and the length-N vector representation of the received signal per information symbol is

$$\mathbf{y} \triangleq \tilde{\mathbf{h}} x + \mathbf{w} \tag{2}$$

where $\mathbf{w} = \begin{bmatrix} w_1 & \ldots & w_N \end{bmatrix}^T \sim \mathcal{CN}(\mathbf{0}_{N\times 1}, \sigma^2 \mathbf{I}_N)$, $\tilde{\mathbf{h}} = \begin{bmatrix} \tilde{h}_1 & \ldots & \tilde{h}_N \end{bmatrix}^T \sim \mathcal{CN}(\mathbf{0}_{N\times 1}, M\mathbf{I}_N)$. Furthermore, variables $\tilde{h}_n \triangleq \sum_{m=1}^{M} h_m^n \exp\{+j2\pi\Delta f_m[(n-1)L + l]T_s\}$, $\forall\ n = 1, \ldots, N$ are i.i.d and proper complex Gaussian random variables $\sim \mathcal{CN}(0, M)$ and $h_m^n \triangleq h_m^{(n-1)L+l} \sim \mathcal{CN}(0,1)$ denotes the channel coefficient of the m^{th} transmitter for the n^{th} element. For proofs and further details on the adopted signal model, we refer the interested reader to [17].

3. EXPERIMENTAL TESTBED SETUP

This section holds the description of our low-cost experimental testbed setup. Fig. 1 depicts two custom-built, embedded, software-controlled transceivers [18] whose synchronized transmission is ensured by a third identical *maestro* node. USRP2, a commercially available SDR developed by Ettus [19], is used as the destination receiver.

3.1. Distributed Transmitters: Low-cost, Custom, Embedded Software-controlled Transceivers

In contrast with previous works on collaborative beamforming, we have employed highly unsynchronized, low-cost, embedded transceivers to play the role of distributed transmitting terminals. Each transceiver consists of a Chipcon/TI CC2500 radio transceiver, interfaced to a Silabs C8051F321 microcontroller unit (MCU). Each node was designed and fabricated in the context of work in [18] and has been given the name *iCube*. iCube's radio operates at the 2.4GHz band. For our implementation On-Off Keying (OOK) modulation was adopted and the transmission rate was set to 2.39kbps.

In accordance with prior art, distributed transmitters achieve packet/symbol level synchronization by assigning the role of the *maestro* to one of the iCube transmitters. Among the three nodes depicted in Fig. 1-(a), $M = 2$ nodes are waiting in "rx" state, listening to $f_{c_1} = 2.457$GHz, while a third node is transmitting a common pilot signal every 1sec at the same frequency. Upon reception of a valid reference packet, distributed transmitters switch into "tx" state and synchronously transmit their information symbols at frequency $f_{c_2} = 2.446$GHz.

iCubes offer a variety of reconfigurable control registers over crucial communication parameters (i.e., transmission rate, power, modulation etc.), allow fast frequency hopping around 2.4GHz band, offer quite small TX/RX switch times (on the order of microseconds) and their overall cost is low. Even though these low-cost, commodity radios, cannot offer explicit carrier synchronization or access to physical layer processing, the aforementioned characteristics allow us to apply the low-complexity protocol for packet synchronization described above. Therefore, there is no need to utilize highly sophisticated SDR devices as collaborative transmitting nodes, and iCubes may be used for evaluating the concept

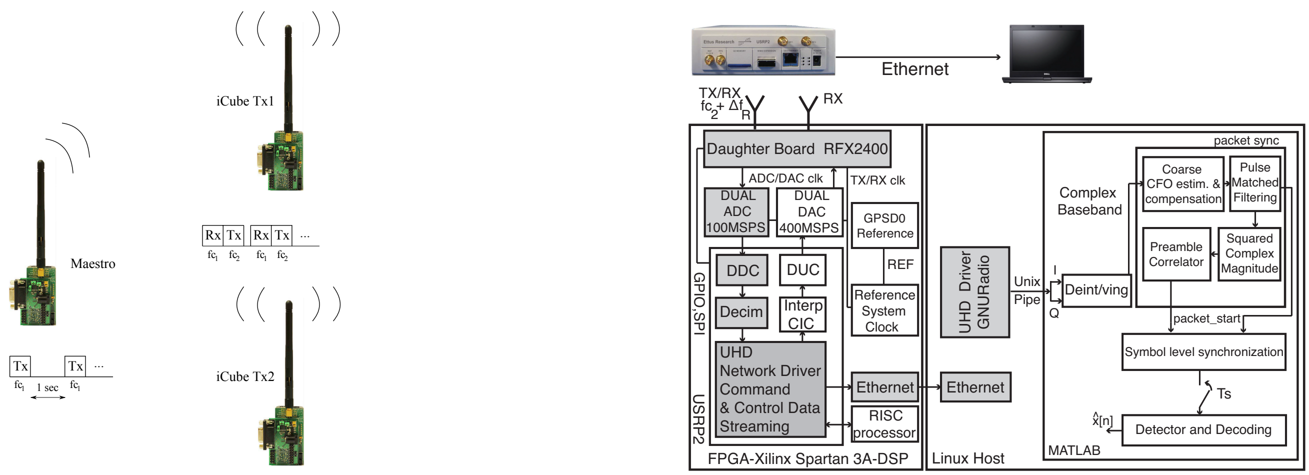

(a) Custom beamforming transmitters (iCube).

(b) Destination receiver's architecture.

Fig. 1. Experimental setup. Beamforming transmitters along with maestro deployed (left), and a commercial SDR USRP2-based destination receiver interfaced to a host Linux-PC (right).

of the proposed *zero-feedback* scheme.

3.2. USRP2 Receiver: Low-cost, Commercial SDR

In the receiver side of our testbed (Fig. 1-(b)), the Universal Software Radio Peripheral (USRP2 version) was utilized. USRP2 is a low-cost, simple and flexible SDR platform that consists of two 14-bit analog-to-digital converters (ADCs), capable of 100MS/s, two 16-bit digital-to-analog converters (DACs), capable of 400MS/s –both attached to a motherboard, a Gigabit Ethernet (GigE) interface and a Xilinx Spartan 3A FPGA which is used for high rate signal processing. The on-board FPGA is used for high-speed digital up and down conversion from baseband to IF, while from IF to RF we use a detachable analog RF daughterboard. In our experiments RFX2400 boards, which offer zero-IF (homodyne) receiver architecture and operate at 2.25-2.9GHz were mounted on USRP2. RFX daughterboards employ quadrature direct downconversion of the received signal to DC, which is then fed to the ADCs for digitization. The FPGA attached to USRP2's motherboard is interfaced to a host computer via GigE. Received baseband IQ data are sent to the PC in the format of 4Bytes per complex sample, therefore the maximum data rate over GigE is $\frac{125\mathrm{MB/s}}{4\mathrm{B/Sample}} \simeq 30\mathrm{MS/s}$ ($25\mathrm{MS/s}$ due to overhead [20]). However, the true maximum sampling rate that the PC can handle depends on its hardware specifications and data processing capabilities. Finally, a decimation rate of 256 was used, providing us with a sampling window of 390.625kHz, which is wide enough to capture the transmitted signals.

Physical layer processing takes place at the host PC by using a free software development toolkit named GNU Radio [21], a host driver and application programming interface called Universal Hardware Driver (UHD) and MATLAB.

4. NON-COHERENT RECEIVERS

In this section, we present the software implementation of a non-coherent receiver (Fig. 1-(b)) that is capable of decoding both transmitted schemes described in Section 2.

First, GNU Radio software is used in order to setup a connection between the USRP2's UHD *source* block and a file *sink* block (FIFO type). Complex IQ samples arriving at the host PC need firstly to be de-interleaved. The next step is to coarsely estimate and correct the frequency offset between receiver and collaborative transmitters. iCube's transceiver operates on its own external oscillator with frequency offsets on the order of 20 parts per million (ppm), while clock instability for USRP2 as reported by Ettus is typically between $10-20$ ppm when the oscillator is not locked.

By calculating the Fourier transform of the fourth power of the received complex baseband signal, $Y(f) = \mathcal{F}\{(y_I(t)+y_Q(t))^4\}$ and finding the frequency where its squared magnitude is maximized $f^* = \arg\max_f \left(|Y(f)|^2\right)$, we get an estimate about how much shifted our received signal is in the frequency axis. After compensating the coarse frequency offset between the receiver and the collaborative transmitters, the start of each packet is estimated by correlating the squared magnitude of the pulse matched filtered signal with an already known preamble sequence. Next, the start of the first symbol is estimated by an energy based approach. Specifically, the pulse matched filtered signal is sampled at rate $1/T_s$ and the energy of all the possible symbol-spaced subsequences is calculated. The sequence with the maximum energy results in a good estimation for the start of the first symbol. Finally, the following non-coherent detectors are applied.

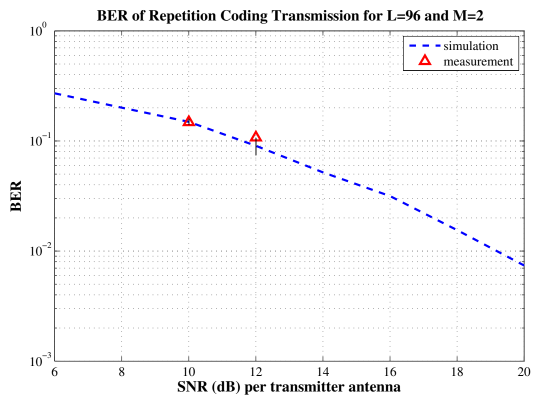

Fig. 2. BER performance for the repetition coding scheme is evaluated with both simulated and experimental data.

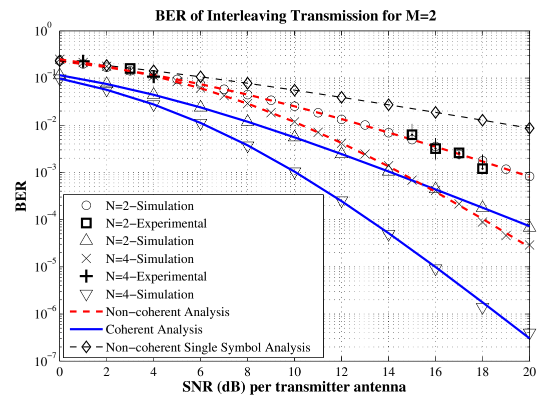

Fig. 3. Experimental matches simulation and analysis BER performance for interleaving transmission in different phases.

4.1. Repetition Coding

Using OOK modulation, and repetition coding for L symbols, the non-coherent binary detector as derived in [17] is $\sum_{l=1}^{L} |y_l|^2 \overset{H_1}{\geq} \theta(k)$, where threshold $\theta(k)$ is set to $\theta(k) \simeq E[w] + k\sqrt{\mathrm{Var[w]}} = \sigma^2 \left(L + k\sqrt{L}\right)$ and parameter k is selected, based on BER minimization, through simulations [17].

4.2. Interleaving

In the case that the adopted transmission technique is interleaving, and assuming equiprobable binary information symbols, the non-coherent maximum-likelihood (ML) binary detector is proved to be the following ([17])

$$||\mathbf{y}||_2^2 \overset{H_1}{\geq} N\frac{\sigma^2(1+2M\,\mathrm{SNR})}{2M\,\mathrm{SNR}}\ln(1+2M\,\mathrm{SNR}) = \Theta, \quad (3)$$

where $M = 2$ denotes the number of beamforming transmitters and $\mathrm{SNR} \triangleq \frac{\mathrm{E}[\mathrm{x}_i^2]}{\mathrm{E}[|\mathrm{w}_i|^2]} = \frac{\mathrm{E}_1}{2\sigma^2}$ is the average SNR per m^{th} transmitter antenna, per i^{th} time slot.

4.3. BER results

Performance of both repetition coding and interleaving schemes was evaluated with simulation as well as experimental measurements from the SDR testbed. The non-coherent receivers implemented for repetition coding and interleaving are assumed to spend the same energy in L and N slots when compared with a system where the transmitted information symbols take only a single slot.

Fig. 2 compares simulation versus experimental results when the repetition coding technique is adopted. Each symbol is repetitively transmitted $L = 96$ times by $M = 2$ transmitters. Different values for the k parameter have been applied to different SNR regimes according to the respective analysis in [17]. Specifically, $k = 1$ is the value that minimizes BER in $6 - 10$dB, while $k = 2$ and $k = 3$ are the appropriate values in the regions of $10 - 16$dB and $16 - 20$dB, respectively. Fig. 2 provides experimental results from the SDR testbed at two SNR values, (10 and 12dB) using different transmit power values and keeping the same topology in the setup. The experiments took place in an indoors RF-cluttering lab environment, with many scatterers and attenuators due to building columns, glass windows, and walls.

Fig. 3 provides BER performance simulation results in the case that the interleaving technique is applied at the beamforming transmitters. Taking advantage of transmitting over independent channels, this method achieves both beamforming gains and diversity. In more detail, Fig. 3 depicts BER performance for $M = 2$ transmitters and different number of distinct phases $N = 2, 4$. Experimental measurements are acquired for the following $\mathrm{SNR} = 3, 15, 16, 17$ and 18dB for $N = 2$, and $\mathrm{SNR} = 1, 4$dB for $N = 4$. Standard deviation error bars for the experimental measurements are also provided. The number of data points is limited mainly because of the testbed indoors nature, the granularity of transmission power change (2dBm) and the considerable amount of time that each measurement required. Bit-error rate performance for ML coherent reception is also depicted for reference purposes. Evidently, for bigger N, we trade BER performance for reception delay, since when $N > 2$, all transmissions need to be completed before reception.

5. CONCLUSION

In sharp contrast with prior research on distributed beamforming, we experimentally validated that such schemes are practically feasible with no use of feedback from the destination. To this end, we designed and deployed an experimental, low-cost SDR testbed. Most importantly, the proposed *zero-feedback* scheme is ideal for critical applications, where feedback communication or CSI acquisition is unreliable. The testbed may be potentialy valuable in further research on detection and coding for zero-feedback distributed beamforming.

6. REFERENCES

[1] J. Uher, T. Wysocki, and B. Wysocki, “Review of distributed beamforming,” *Journal of Telecommunications and Information Technology*, 2011.

[2] Y.-S. Tu and G. Pottie, “Coherent cooperative transmission from multiple adjacent antennas to a distant stationary antenna through AWGN channels,” in *Proc. IEEE Vehicular Technology Conf. (Spring)*, May 2002, pp. 130–134.

[3] R. Mudumbai, G. Barriac, and U. Madhow, “On the feasibility of distributed beamforming in wireless networks,” *IEEE Trans. Wireless Commun.*, vol. 6, no. 5, pp. 1754–1763, May 2007.

[4] F. Quitin, M. Mahboob, R. Mudumbai, and U. Madhow, “Distributed beamforming with software-defined radios: Frequency synchronization and digital feedback,” to appear in *IEEE Globecom 2012*.

[5] M. M. U. Rahman, H. E. Baidoo-Williams, S. Dasgupta, and R. Mudumbai, “Fully wireless implementation of distributed beamforming on a software defined radio platform,” in *the 11th ACM/IEEE Conference on Information Processing in Sensor Networks (IPSN 2012)*, 2012.

[6] F. Quitin, U. Madhow, M. Mahboob, and R. Mudumbai, “Demonstrating distributed transmit beamforming with software defined radios,” *IEEE International Symposium on a World of Wireless, Mobile and Multimedia Systems*, Jun. 2012.

[7] M. Seo, M. Rodwell, and U. Madhow, “A feedback-based distributed phased array technique and its application to 60-ghz wireless sensor network,” in *Proc. IEEE Int. Microwave Symposium*, Jun. 2008, pp. 683–686.

[8] M. Johnson, K. Ramchandran, and M. Mitzenmacher, “Distributed beamforming with binary signaling,” in *Proc. IEEE Int. Symp. on Inform. Theory*, Jul. 2008, pp. 890–894.

[9] V. Havary-Nassab, S. Shahbazpanahi, A. Grami, and Z.-Q. Luo, “Distributed beamforming for relay networks based on second-order statistics of the channel state information,” *IEEE Trans. Signal Processing*, vol. 56, no. 9, pp. 4306–4316, Sep. 2008.

[10] Y. Jing and H. Jafarkhani, “Beamforming in wireless relay networks,” in *Proc. Inf. Theory Appl. Worksh.*, 2008, pp. 142–150.

[11] Y. Zhang, X. Li, and M. Amin, “Distributed beamforming in multi-user cooperative wireless networks,” in *Proc. 4th Int. Conf. Commun. Network. China (ChinaCOM)*, Aug. 2009, pp. 1–5.

[12] N. Zhang, G. Kang, Y. Guo, P. Zhang, and X. Gui, “Adaptive transmitted distributed antenna selection strategy in distributed antenna systems with limited feedback beamforming,” *Electron. Lett.*, vol. 45, no. 21, pp. 1079–1081, Oct. 2009.

[13] R. Mudumbai, J. Hespanha, U. Madhow, and G. Barriac, “Distributed transmit beamforming using feedback control,” *IEEE Trans. Inform. Theory*, vol. 56, no. 1, pp. 411–426, Jan. 2010.

[14] D. Brown and H. Poor, “Time-slotted round-trip carrier synchronization for distributed beamforming,” *IEEE Trans. Signal Processing*, vol. 56, no. 11, pp. 5630–5643, Nov. 2008.

[15] I. Ozil and D. Brown, “Time-slotted round-trip carrier synchronization,” in *Proc. of the 41st Asilomar Conference on Signals, Systems, and Computers*, Nov. 2007, pp. 1781–1785.

[16] A. Bletsas, A. Lippman, and J. Sahalos, “Simple, zero-feedback, distributed beamforming with unsynchronized carriers,” *IEEE J. Select. Areas Commun.*, vol. 28, no. 7, pp. 1046–1054, Sep. 2010.

[17] K. Alexandris, “Distributed zero-feedback beamforming for emergency radio,” Diploma Thesis, Technical University of Crete, Chania, Greece, Sep. 2012, http://users.isc.tuc.gr/~kalexandris/theses.html.

[18] A. Bletsas, A. Vlachaki, E. Kampianakis, J. Kimionis, G. Sklivanitis, K. Tountas, M. Asteris, and P. Markopoulos, “Building the low-cost digital garden as a telecom lab exercise,” *IEEE Pervasive Computing*, vol. 12, no. 1, pp. 48–57, Jan.-Mar. 2013.

[19] (2012) USRP products. Matt Ettus. [Online]. Available: http://www.ettus.com

[20] (2012) USRP products. Matt Ettus. [Online]. Available: http://www.ettus.com/content/files/kb/application_note_distributed_rf_sensors.pdf

[21] (2012) GNU radio. [Online]. Available: http://gnuradio.org/redmine/projects/gnuradio/wiki